Control of Bond Excitation and Dissociation in HCN Using Laser Pulses†

Richard Brezina and Wing-Ki Liu*

Department of Physics and Guelph-Waterloo Physics Institute, University of Waterloo, Waterloo, Ontario, Canada N2L 3G1

Received: March 9, 2004; In Final Form: May 20, 2004

The potential for selectively controlling the excitation and dissociation of the two bonds of the linear triatomic molecule HCN using short laser pulses is studied. We show that intramolecular vibrational redistribution (IVR) has strong influence on the controlling process: at low excitation level, IVR is slow and it is easy to control the excitation of either bond, whereas at higher exitation, IVR causes rapid leakage into the unexcited bond, making control more difficult. Simple linearly chirped pulses are effective in exciting and dissociating the weaker C−H bond. In an attempt to excite the stronger C−N bond, we found that although linearly chirped pulses can transfer energy to the C−N bond, they cannot compete with the much faster internal energy redistribution, and the C−N bond cannot be dissociated because the weaker C−H bond will always break first. To overcome this problem, we construct an optimization scheme and use it to find pulses that do effect C−N dissociation. These pulses however are very short (less than 0.5 ps) and too intense (with brief peaks in the low 10^{15} W/cm^2 range) so that the molecule will be ionized before dissociation into neutral fragments can occur.

I. Introduction

The invention of the laser has inspired the hope of using coherent light to control the pathways of chemical reactions by selectively exciting a specific bond vibrationally.[1] Early experiments on multiphoton vibrational excitation using nanosecond laser pulses encountered the problem of intramolecular vibrational redistribution (IVR) which occurs on the picosecond scale, making selective excitation difficult. Recently, the availability of high-intensity femtosecond (fs) lasers and advances in pulse shaping techniques enable the experimentalists to control the phase and amplitude of light over a large spectral bandwidth.[2,3] Employing a closed loop learning algorithm, selective breaking and rearrangement of chemical bonds in polyatomic molecules have been demonstrated,[4] and selective excitation and suppression of vibrational modes in molecular gases have been achieved.[5] The shape of the optimal pulse obtained from such learning control loops can be rather complicated. Earlier, using mid-infrared (MIR) fs pulses from a free-electron laser with a linear chirp,[6−8] gas-phase NO molecules have been selectively excited to vibrational levels $v \leq 5$. Recently, linearly chirped MIR pulses were obtained from propagating fs laser pulses, generated by difference frequency mixing of the signal and idler pulses of an optical parametric amplifier, through dispersive materials. Using these chirped pulses, ground-state dissociation of CO from transition metal carbonyl molecules can be controlled by selective excitation of the CO stretch of the molecules.[9,10]

Theoretical studies of selective laser excitation have also been an active area of research in the past decade.[11−20] Chelkowski et al.[11] were the first to show, from a quantum mechanical simulation of the interaction of the diatomic molecule HF with a linearly chirped laser pulse, that efficient vibrational ladder climbing leading ultimately to dissociation can be achieved at laser intensities below the ionization threshold. Subsequently, a classical description of chirped pulse excitation in terms of the so-called "bucket dynamics" was given.[21] To understand the dynamics of laser−molecule interactions, most of these theoretical studies treat the simple case of a diatomic molecule in a radiation field. Usually, the vibration of the diatomic molecule is modeled by a Morse oscillator[22,23] which is the simplest (but realistic) anharmonic oscillating system that can be solved exactly both quantum mechanically and classically. Of course, the problem of IVR does not arise in diatomic molecules, and the simplest system that IVR can interfere with selective excitation is a triatomic molecule. In the quantum mechanical study of the interaction of an HCN molecule with ultrashort chirped infrared laser pulses,[12,24] it was shown that properly chosen chirped pulses are effective in exciting and dissociating the weaker C−H bond and in controlling the excitation of the stronger C−N bond. Selectivity has also been demonstrated for the molecular ion system of the type ABC^+ using intense infrared laser pulses.[25] The selective photodissociation of the stronger C−N bond in the HCN molecule has been investigated based on classical optimal control theory.[26] However, the optimal IR pulses so obtained are rather complicated. In this paper, we study classically the photoexcitation of HCN and the effects of IVR on the dynamics of excitation and dissociation. To understand the interaction of the molecule with an intense IR pulse, for most of our study, we choose a simple form of the laser pulse with a linear frequency chirp, which can readily by produced in the laboratory.[10,27] Recently, a clever scheme was proposed[28] in which an optical centrifuge consisting of two off-resonant oppositely chirped and counter-rotating laser pulses forces the HCN molecule to rotate rapidly, eventually leading to the breaking of the strong C−N bond between the heavier nuclei of the molecule. During the rotational acceleration, there is little vibrational excitation. In our study, we consider direct resonant excitation of the intramolecular bond. We ignore rotation by employing a linear model, which can be

† Part of the "Gert D. Billing Memorial Issue".

* To whom correspondence should be addressed.

10.1021/jp0489370 CCC: $27.50 © 2004 American Chemical Society
Published on Web 06/30/2004

partly justified by the fact that a high intensity, linearly polarized laser field tends to align the molecule along the direction of the polarization.[29]

In section II, we give a brief discussion of our linear model of the HCN molecule including the intramolecular potential, the transition dipole moment, and the interaction with the electric field of the laser pulse. In section III, we summarize the quasiclassical trajectory method that we employed in our calculation. We then present in section IV representative results of our computations, which include data on the excitation and dissociation of both the C−H and C−N bonds of the molecule by various laser pulses. We conclude in section V by discussing the significance of these results and their possible applications toward selective bond excitation of the HCN molecule.

II. Model of HCN Interacting with Laser Field

We model the HCN molecule as a system of two kinetically coupled Morse oscillators, interacting with an external electric field through its electric dipole moment. This dipole moment function is dependent on the stretching coordinates of each bond. We assume the molecule to be nonrotating, linear, and aligned with the electric field of a linearly polarized laser. Strictly speaking, the C−H stretch is coupled to the bending mode, and it has been shown that isomerization of HCN can be induced by intense infrared laser pulses.[30] Such coupling would give rise to additional IVR, but for simplicity, we ignore the bending motion in this study.

The Hamiltonian for our system can be written as

$$H = H_{CH}(X, P_X) + H_{CN}(Y, P_Y) + T_C(P_X, P_Y) + H_{int}(X, Y, t) \tag{1}$$

where

$$H_{CH}(X, P_X) = \frac{1}{2\mu_{CH}} P_X^2 + D_{CH}(1 - e^{-aX})^2 \tag{2}$$

and

$$H_{CN}(Y, P_Y) = \frac{1}{2\mu_{CN}} P_Y^2 + D_{CN}(1 - e^{-bY})^2 \tag{3}$$

are the kinetic and potential energy terms for each bond

$$T_C(P_X, P_Y) = -\frac{1}{m_C} P_X P_Y \tag{4}$$

is the kinetic coupling term between the bonds, and

$$H_{int}(X, Y, t) = -\mu(X, Y)\, E_L(t) \tag{5}$$

represents the electric dipole interaction with the time dependent laser electric field $E_L(t)$. In the above equations, X and Y are the deviations of the C−H and C−N bond coordinates from their equilibrium values, P_X and P_Y are their corresponding conjugate momenta, μ_{CH} and μ_{CN} are the reduced masses of the C−H and C−N bonds, D_{CH} and D_{CN} the respective Morse well depths, a and b the respective Morse constants, and m_C the mass of the central carbon atom. The transition dipole moment function $\mu(X, Y)$ for HCN has been computed using ab initio methods for selected points near the equilibrium configuration.[31] We have used these ab initio results to fit a function of the following form:

$$\mu(X, Y) = e^{-\gamma(X+X_e)} \sum_{i=1}^{4} A_i (X + X_e)^i + e^{-\gamma(Y+Y_e)} \sum_{i=1}^{4} B_i (Y + Y_e)^i \tag{6}$$

where X_e and Y_e are the equilibrium bond lengths of C−H and C−N, respectively, and γ is chosen to be 1 bohr^{-1}. The numerical values of the molecular parameters used in our calculation are summarized in Table 1.

TABLE 1: Molecular Parameters for HCN

symbol	value	units	parameter
a	1.847393	Å^{-1}	Morse parameter of C−H bond
b	2.306172	Å^{-1}	Morse parameter of C−N bond
D_{CH}	5.69714	eV	well depth of C−H bond
D_{CN}	10.99446	eV	well depth of C−N bond
X_e	1.065493	Å	equilibrium C−H bond length
Y_e	1.153209	Å	equilibrium C−N bond length
d_{CH}	1.11806	D/Å	equilibrium C−H dipole moment derivative
I_0	1.0853×10^{17}	W/cm^2	laser−molecule coupling parameter
$\hbar\omega_{CH}$	0.4181	eV	quantum of C−H vibrational energy
$\hbar\omega_{CN}$	0.2750	eV	quantum of C−N vibrational energy
$1/\omega_{CH}$	1.5743	fs	unit of time
$\hbar_{eff}$	0.0366945		effective Planck's constant
a	1.24834		reduced Morse parameter of C−N bond
D	1.92982		reduced well depth of C−N bond
μ_c	12.9169		relative mass of C atom
μ_y	6.9583		relative reduced mass of C−N bond
i_d	2.9345		reduced action of C−N bond at dissociation
N_{CH}	27		number of bound states of C−H bond
N_{CN}	80		number of bound states of C−N bond

In our calculation, we define dimensionless quantities by scaling the dynamical variables with respect to the Hamiltonian to the C−H bond. Thus energy is scaled by $2D_{CH}$, time is scaled by $1/\omega_{CH} = (2D_{CH}a^2/\mu_{CH})^{1/2}$, the inverse of the harmonic vibrational frequency of the C−H bond, and length is scaled by the inverse Morse parameter $1/a$. Writing the electric field of the laser pulse as

$$E_L(t) = E_0 U(t) \cos \Phi(t) \tag{7}$$

where E_0 is the field amplitude, $U(t)$ is a dimensionless envelope function, and $\Phi(t)$ is the phase of the laser field so that the instantaneous frequency is given by $\omega(t) = d\Phi(t)/dt$, the laser−molecule interaction energy is characterized by the constant[21,32]

$$B = \frac{d_{CH} E_0}{2aD_{CH}} \tag{8}$$

where

$$d_{CH} \equiv \frac{\partial \mu}{\partial X}(0, 0)$$

is the effective charge of the C−H bond. Thus B is related to the intensity I of the laser by $I = I_0 B^2$ where $I_0 = (c/8\pi)(2aD_{CH}/d_{CH})^2$. With the reduced Hamiltonian defined by $h \equiv H/2D_{CH} = h_x + h_y + t_c + h_{int}$, where

$$h_x = \frac{1}{2} p_x^2 + \frac{1}{2}(1 - e^{-x})^2 \tag{9}$$

$$h_y = \frac{1}{2\mu_y} p_y^2 + \frac{1}{2} D(1 - e^{-\alpha y})^2 \tag{10}$$

$t_c = -p_x p_y/\mu_C$ and $h_{int} = -B\mu_d(x, y)U(\tau)$, the Hamilton's

TABLE 2: Parameters for Dipole Moment Derivatives of HCN

i	1	2	3	4	5
a_{xi}	1.000000	1.037553	0.025501	−1.509024	−0.399062
a_{yi}	−0.292937	−1.460587	−1.194040	0.849744	0.429321

equations for the dimensionless variables then take the form

$$\frac{dp_x}{d\tau} = -(1 - e^{-x})e^{-x} + B\frac{\partial}{\partial x}\mu_d(x, y)U(\tau)\cos\Phi(\tau) \quad (11)$$

$$\frac{dx}{d\tau} = p_x - \frac{1}{\mu_c}p_y \quad (12)$$

$$\frac{dp_y}{d\tau} = -D\alpha(1 - e^{-\alpha y})e^{-\alpha y} + B\frac{\partial}{\partial y}\mu_d(x, y)U(\tau)\cos\Phi(\tau) \quad (13)$$

$$\frac{dy}{d\tau} = \frac{1}{\mu_y}p_y - \frac{1}{\mu_c}p_x \quad (14)$$

where ($x = aX$, $y = aY$) are the dimensionless bond coordinates with corresponding dimensionless conjugate momenta (p_x, p_y), $\tau = \omega_{CH}t$ is the dimensionless time, $\mu_y \equiv \mu_{CN}/\mu_{CH}$, $\mu_c \equiv m_c/\mu_{CH}$, $\alpha \equiv b/a$, and $D \equiv D_{CN}/D_{CH}$. The dimensionless dipole moment function is given by

$$\mu_d(x, y) = \frac{a}{d_{CH}}\mu(X, Y) \quad (15)$$

and since it is the derivatives of the dipole moment function that enter in eqs 11 and 13, we use the following expansions obtained from eq 6:

$$\frac{\partial\mu_d}{\partial x} = e^{-\alpha x}(a_{x1} + a_{x2}x + a_{x3}x^2 + a_{x4}x^3 + a_{x5}x^4) \quad (16)$$

where $\alpha = 1.022915$ and a similar expression for $\partial\mu_d/\partial y$. These coefficients are given in Table 2.

III. Quasiclassical Trajectory Method

The classical Hamilton's equations (11−14) can readily be integrated numerically once the initial conditions are chosen. We create the classical analogue of the zeroth order quantum vibrational states (n_{CH}, n_{CN}) of the molecule according to the Born−Sommerfeld quantization rule[33] by quantizing the classical actions of the zeroth order Hamiltonians H_{CH} and H_{CN} and assigning to each bond the initial action values of

$$\left(n_{CH} + \frac{1}{2}\right)\hbar$$

and

$$\left(n_{CN} + \frac{1}{2}\right)\hbar.$$

We ignore the contribution of the coupling term.

For a Morse oscillator in dimensionless units (the zeroth order Hamiltonian for the C−H bond, eq 9), the transformations between the action-angle variables (i,θ) and the Cartesian coordinates (x, p_x) can be derived from classical canonical transformation theory:[23,34]

$$x = \ln\frac{1 - \sqrt{1 - (1 - i)^2}\cos\theta}{(1 - i^2)} \quad (17)$$

$$p_x = \frac{\omega\sqrt{1 - \omega^2}\sin\theta}{1 - \sqrt{1 - \omega^2}\cos\theta} \quad (18)$$

$$h_x(i) = \frac{1}{2}[1 - (1 - i)^2] \quad (19)$$

with the classical frequency given by

$$\omega = \frac{\partial h_x}{\partial i} = 1 - i. \quad (20)$$

The Born-Sommerfeld quantization condition becomes

$$i^{(n)} = \left(n + \frac{1}{2}\right)\hbar_{eff}, \quad n = 0, 1, 2, ... \quad (21)$$

where $\hbar_{eff}$ is the effective Planck constant

$$\hbar_{eff} = \frac{a}{\sqrt{2\mu_{CH}D_{CH}}}\hbar = \frac{\hbar\omega_{CH}}{2D_{CH}} \quad (22)$$

The quantum state n is then represented in the quasiclassical trajectory method by an ensemble of phase space coordinates with classical action given by eq 21 and angles uniformly distributed between 0 and 2π. These equation can be directly applied to the C−H bond to generate a set of initial conditions for (x, p_x). For the C−N bond, we make the substitutions in eqs 17−19

$$\frac{p_y}{\sqrt{D\mu_y}} \rightarrow p_x, \quad \alpha y \rightarrow x, \quad \frac{h_y}{D} \rightarrow h_x, \quad \frac{i_y}{i_d} \rightarrow i \quad (23)$$

where

$$i_d = \frac{\sqrt{\mu_y D}}{\alpha} \quad (24)$$

is the dissociation value of the action for the C−N bond (the C−H bond dissociates at $i = 1$ with the scaling we have chosen). Thus, the scaled C−N Hamiltonian is

$$h_y = \frac{1}{2}D\left[1 - \left(1 - \frac{i_y}{i_d}\right)^2\right] \quad (25)$$

yielding the classical frequency $\omega_y = \partial h_y/\partial i_y = (D/i_d)(1 - i_y/i_d)$. The Born-Sommerfeld quantization condition remains unchanged: $i_y^{(n)} = (n + 1/2)\hbar_{eff}$.

Thus, for a given initial vibrational state (n_{CH}, n_{CN}), we calculate the initial actions for the C−H and C−N bonds according to the Born-Sommerfeld quantization condition eq 21 and select a uniform distribution for both the classical angles. These initial values are then converted to the Cartesian variables using the forward transformation eqs 17 and 18, and the appropriate substitutions (23). The ensemble is then propagated

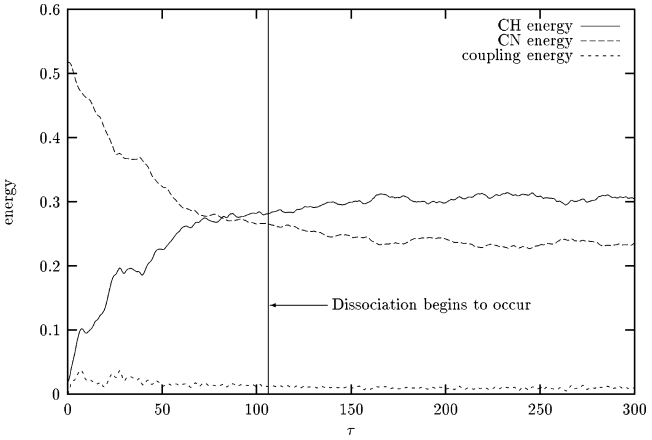

Figure 1. Spontaneous energy redistribution for initial states with $n_{CN} = 25$, $n_{CH} = 0$. The total internal energy of the molecule exceeds the C−H dissociation threshold, and numerous dissociations occur after about 100 time units or 0.15 ps. All observables in the figures are phase-averaged values for an ensemble with 1089 trajectories.

in time by integrating the Hamilton's equations (11−14) using the Bulirsch-Stoer method.[35]

IV. Computational Results

A. Intramolecular Vibrational Redistribution. To help us understand the detailed behavior of the molecule during laser excitation, we first study the spontaneous relaxation of asymmetrically excited states. The average magnitude of the kinetic coupling between the bonds increases with the excitation level of each bond. Energy is thus transferred more readily between the bonds when either bond becomes excited, giving rise to the process of intramolecular vibrational redistribution (IVR), which is of great importance when it comes to selective control of bond excitation. It has been found theoretically[25] that selective excitation can be achieved for pulses whose time scale is comparable to that of the IVR for a given molecule. On longer time scales, we may anticipate that achieving selective dissociation may be considerably more difficult.

We investigate the nature of IVR in the HCN molecule by observing the behavior of the molecule when initially one bond is at its ground-state level, whereas the other bond is at an excited level. The system is then propagated without external perturbation to show the effects of energy redistribution. When the C−H bond is initially prepared at the excited state $n_{CH} = 25$, energy redistribution takes place during about 100 time units. Although the C−H bond begins at an energy very near dissociation, the C−N bond with its deeper potential easily absorbs the excess C−H energy without dissociating. Similar, albeit somewhat slower redistribution behavior is observed for all n_{CH} greater than 15. Below this threshold, the coupling evidently is not large enough to cause complete redistribution, and the energy shows quasiperiodic behavior with very long relaxation times. When the C−N bond is prepared in an excited state, for $n_{CN} \leq 15$, we observe again long-lived, quasiperiodic behavior. Above this threshold, however, IVR "turns on" and relaxation is rapid. A representative case with $n_{CH} = 0$ and $n_{CN} = 25$ is illustrated in Figure 1. This initial state has total energy larger than the dissociation energy of the C−H bond, and not surprisingly, redistribution is accompanied by C−H dissociation with nearly 100% probability. The onset of the dissociation occurs after 100 time units or about 0.15 ps.

The overall behavior of the unperturbed system gives us an indication of two phenomena that are very relevant to our goals of controlled selective dissociation: (1) selective C−H bond dissociation can be achieved quite easily by energy input into either or both bonds and (2) selective C−N bond dissociation can probably be achieved only by selective pumping of this bond on a fast time scale (on the order of 150 fs or faster).

B. Vibrational Excitation by Linearly Chirped Pulses. We next investigate the effects of linearly chirped pulses on the molecule. The chirped pulse is modeled by setting the envelope function $U(t)$ of eq 7 to a unit square pulse of duriation T_p and the phase by

$$\Phi(t) = \Omega_0 t\left[1 - \frac{\alpha_c t}{2T_p}\right] \tag{26}$$

so that the instantaneous frequency becomes

$$\Omega_{ins}(t) = \Omega_0\left[1 - \alpha_c\left(\frac{t}{T_p}\right)\right] \tag{27}$$

Note that $\Omega_{ins}(T_p) = \Omega_0(1 - \alpha_c)$ and hence α_c represents the fractional decrease of the instantaneous frequency at the end of the pulse. $\Omega_{ins}(t)$ is assumed to be a slowly varying function of time compared to $E_L(t)$. In our studies, Ω_0 is set equal to the harmonic frequency of the selected bond, whereas the laser intensity $I = cE_0^2/8\pi$ remains constant for the duration of the pulse. Our choice is motivated by earlier theoretical work[11,21,32] which showed that such pulses can be effective in dissociating diatomic molecules by a process known as "bucket dynamics". Essentially, this process works because the pulse remains resonant with the vibration of the bond as its excitation level increases and its vibrational freqency decreases due to the anharmonicity of the bond. The details of the time rate of change of the laser frequency turn out to have minimal bearing on the efficiency of the excitation process, as long as the decrease is gradual enough. Furthermore, laser pulses with a linear chirp can readily be prepared in the laboratory.[10,27] We therefore adopt the linearly chirped pulse because of its relative simplicity.

Since the kinetic coupling between the bonds represents only a minor perturbation at low excitation levels of the molecule, the bonds behave in a nearly independent manner, and we would expect that the bucket dynamics description for diatomic molecules[20,21,32] should apply quite well to either bond. We begin with the molecule in its ground state and tune the initial frequency of the pulse to the harmonic frequency of the bond we are targeting. We can choose the amount of chirping (determined by the parameter α_c in eq 27) to be fairly small so that the final state and all intermediate states remain within the low excitation regime.

Figures 2 and 3 show typical pumping to a low excited state of the C−H and C−N bond, respectively. In each case, $n \simeq 10$ was the target excitation state; for this purpose, the pulse chirping was from $\Omega_{ins} = 1.00$ to 0.64 (measured in units of the C−H harmonic frequency) for the C−H bond and from $\Omega_{ins} = 0.63$ to 0.56 for the C−N bond. We observe that pumping takes place much as predicted by bucket dynamics, with the characteristic oscillatory increase in excitation, for each bond. These oscillations can be explained by the appearance of local minima in the effective potential in a moving frame in phase space; these are the so-called buckets.[21,32] Trajectories can become trapped there, and oscillate about the minima. It is these oscillations that appear in the figures, superimposed over the uniform "convective" motion of the bucket. Oscillations are most pronounced near the beginning of the pulse and decay thereafter. During the excitation of the C−H bond, we observed in Figure 2 that a pronounced increase in the C−N energy takes place at $\tau > 1000$; this is most likely due to energy redistribution as energy leaks from the highly excited C−H bond.

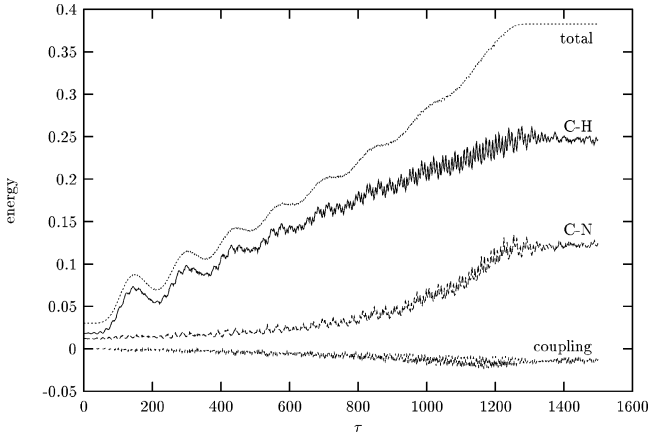

Figure 2. Excitation of the C−H bond to the $n \simeq 10$ level by a resonant chirped pulse. Oscillations within the bucket trap are visible for $\tau < 500$. The C−N bond begins to pick up energy at $\tau \sim 1000$; this is due to IVR and also due to an accidental resonance with the pulse frequency which approaches the C−N harmonic frequency of 0.67 near the end of the pulse. The parameters of the pulse are intensity 1×10^{13} W/cm^2; duration 1300; frequency sweeps from 1.0 to 0.64.

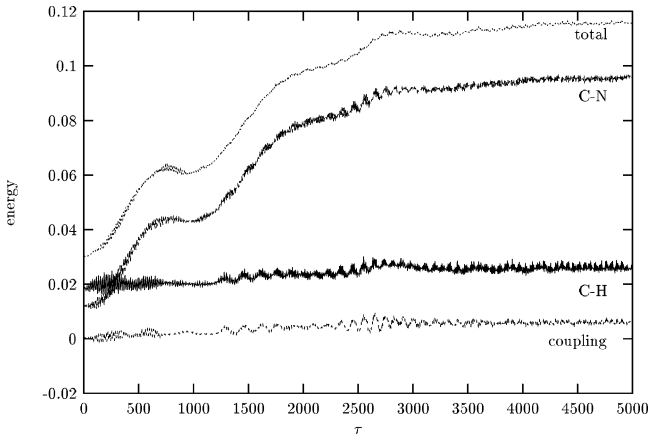

Figure 3. Excitation of the C−N bond to the $n \simeq 10$ level by a resonant chirped pulse. The pulse parameters are intensity 1×10^{14} W/cm^2; duration 5000; frequency sweeps from 0.63 to 0.56. Compared with the weaker C−H bond, much longer pulse durations and higher intensities are required to excite the heavier, stronger C−N bond.

For the pumping of the C−N bond in Figure 3, a comparatively longer pulse is required; this is due to the deeper potential well for this bond, as well as its greater reduced mass. Higher laser intensity is required as well; a factor here is the smaller C−N transition dipole moment and, consequently, reduced coupling to the electric field. Oscillations within the bucket are clearly visible and are much slower than the C−H case. The C−H bond remains quiescent throughout; the level of C−N excitation is insufficient to cause IVR, and no accidental resonances with the C−H bond occur.

Since the bond energies shown in these figures are ensemble averages, the graphs do not show explicitly the relative proportion of trajectories that have been captured by the buckets. A closer inspection of the data reveals that in fact about 80% of the trajectories have been captured in the C−H excitation of Figure 2, whereas about 40% of the trajectories were captured in the C−N excitation of Figure 3. We conclude that bucket dynamics is efficient at changing the energy of either bond selectively, at relatively low excitation energies. We may expect this process to break down, however, once the kinetic coupling in the molecule becomes more important at higher excitation levels. In the C−H case, this process is already in evidence,

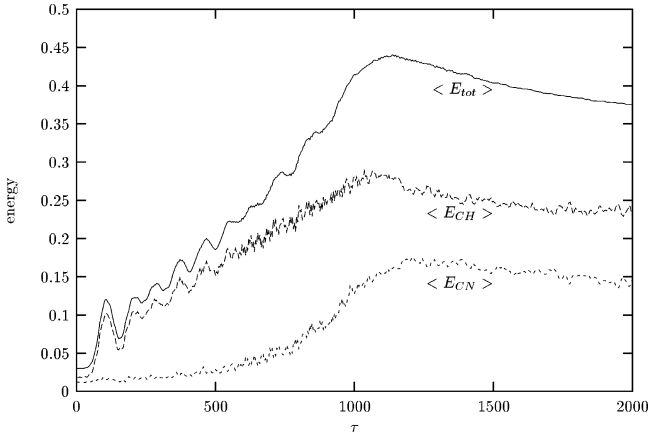

Figure 4. Sample plot of an efficient excitation of the C−H bond with a linearly chirped pulse. Note the oscillations within the convective bucket as evidenced by fluctuations in the internal energy of the C−H bond.

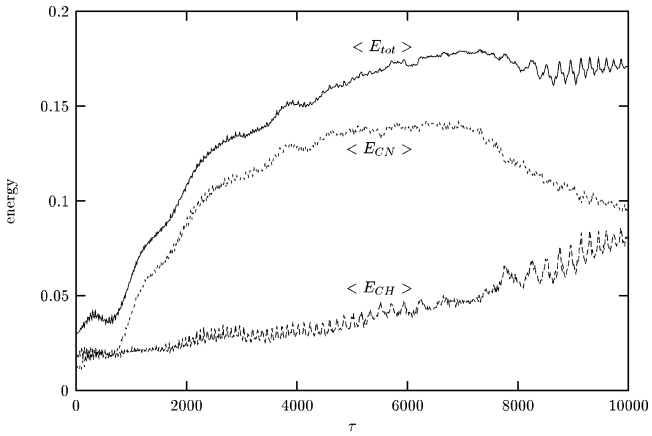

Figure 5. Sample plot of an attempt at exciting the C−N bond with a linearly chirped pulse. Initially a bucket captures some trajectories but these are lost as energy is redistributed into both bonds.

and in fact, only about 20% of the C−N trajectories remain near the ground state at the end of the pulse.

C. Dissociation by Linearly Chirped Pulses. We found that linearly chirped pulses, with a proper choice of pulse parameters, can indeed excite either bond of the molecule, although excitation of the C−N bond required relatively higher intensitites and longer pulse durations. However, once the bond reaches a sufficiently high excitation level (approximately $n > 15$, well below dissociation for either bond), IVR takes place and although the weaker C−H bond may eventually break, the excitation is no longer selective. The stronger C−N bond, on the other hand, never dissociates at laser intensities of less than 10^{15}W/cm^2. At such high intensities, the molecule will become ionized before dissociation into neutral fragments can occur.

Figure 4 shows the time development of the excitation of the C−H bond with laser intensity $I = 5 \times 10^{13}$W/cm^2, pulse duration $T_p = 1800$, and final frequency $\Omega_{ins}(T_p) = 0.5$ which is resonant with the $n = 14$ state of the C−H bond. This laser pulse is sufficient to ensure that most of the trajectories dissociate, and dissociations begin to occur near $\tau = 1000$. We can also see some secondary excitation of the C−N bond due to coupling of the bond to the laser when the frequency sweeps down through its ground-state resonance at $\omega_y = 0.66$. Internal energy redistribution may also be a factor in causing this C−N excitation.

In Figure 5, we display a typical example of the excitation of the C−N bond with a chirped pulse of intensity $I = 2 \times$

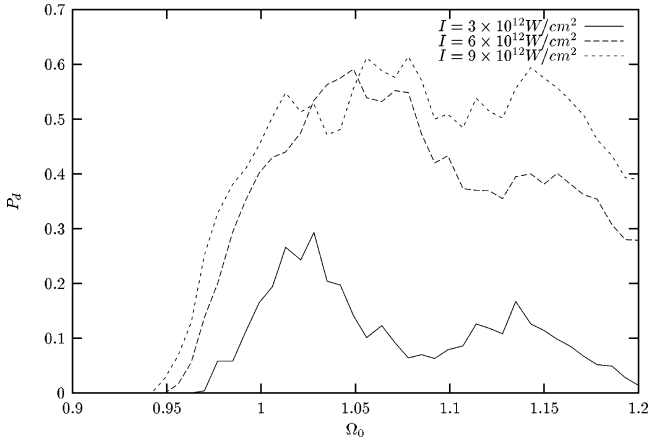

Figure 6. C−H dissociation probability as a function of initial pulse frequency for laser intensities in the 10^{12} W/cm^2 range. Note the threshold behavior at frequencies just under the resonant frequency $\Omega_0 = 1.0$.

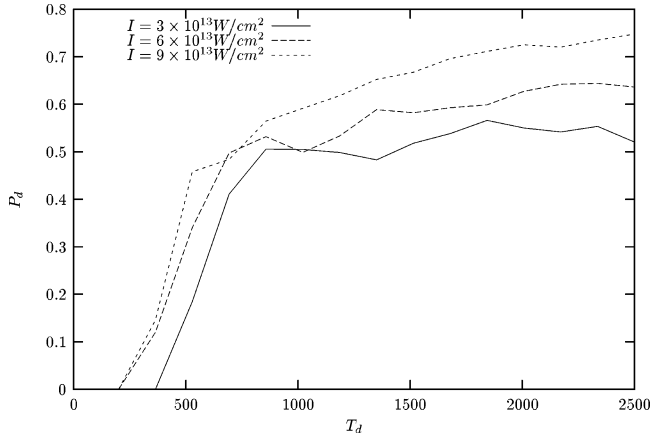

Figure 7. Dependence of the C−H dissociation probability P_d on pulse duration T_d. Note the threshold at $T_d \sim 500$ and the flat response for $T_d > 1000$ once saturation is reached.

10^{14} W/cm^2, duration $T_p = 10\,000$, and final frequency $\Omega_{ins}(T_p) = 0.45$ which is resonant with the $n = 22$ state of the C−N bond. Here, we observe the breakdown of the selective pumping process which happens well short of dissociation. The excitation stops at $\tau \sim 7000$ when energy rapidly leaks into the C−H bond as evidenced by a corresponding increase in the C−H bond internal energy. Another factor contributing to the increase in C−H energy is a second-order resonance when the pulse frequency sweeps past 0.5. The C−H bond energy of some trajectories reaches its dissociation value at $\tau \sim 7000$, and thereafter, C−H dissociation begins to occur. We could not find a physically reasonable combination of the parameters of a linearly chirped pulse that would not result in a similar outcome. It seems that it is not possible to produce dissociations or highly excited levels of the C−N bond without inevitably breaking the weaker C−H bond first, at least with pulses on time scales much longer than a few vibrational periods of the bonds.

The simple linearly chirped pulse is thus effective only for dissociating the C−H bond. Its simplicity, however, makes it useful in the laboratory. We therefore present some additional results about the efficacy of this pulse. Specifically, we investigate the ranges of pulse parameters (laser intensity, intial frequency, and pulse duration) for which a linear chirped pulse is effective in transferring energy to the HCN molecule and dissociating the C−H bond. Because we wish to study the dissociation dynamics of the C−H bond, we choose a chirped pulse with a large value of $\alpha_c \simeq 0.5$ and use the probability of dissociation as a gauge of pulse effectiveness. The molecule begins in the ground state at $\tau = 0$ as the pulse is turned on, and the quantities plotted are all averages over an ensemble of 1089 trajectories. Figure 6 shows the dependence of the dissociation probability on the initial pulse frequency measured in units of the C−H harmonic frequency. Three graphs are shown for different values of laser intensity. The pulse duration was 1700 time units which ensured a slow enough chirping rate for excitation to proceed. As expected, from resonance considerations, a threshold exists near $\Omega_0 = 1.0$, with some resonance structure observed as Ω_0 increases. On the other hand, probabilities of dissociation quickly go to zero below $\Omega_0 = 0.95$. The effectiveness of the pulse generally increases with increasing laser intensity, although saturation occurs at intensities close to 6×10^{12} W/cm^2. The saturated dissociation probabilities hover in the vicinity of 0.5. The threshold frequency decreases with increasing intensity, from about $\Omega_0 = 0.97$ for 3×10^{12} W/cm^2 to about $\Omega_0 = 0.93$ for 3×10^{13} W/cm^2.

Next we study the dependence of the C−H dissociation probability on the pulse duration, which is inversely proportional to the chirping rate since we fix the value of $\alpha_c = 0.5$ (see eq 27) and all of the 1089 molecules in the ensemble begin in the ground state. Figure 7 shows the probabilities of dissociation for three intensities in the 10^{13} W/cm^2 range. Dissociations begin occurring for pulses about 300 time units in length, and saturation occurs by 900 time units. The dependence on intensities is relatively weak, with the onset of dissociation occurring slightly earlier and the saturation levels becoming somewhat higher, for the more intense pulses. Saturation probabilities are in the neighborhood of 0.5−0.7 and increase only slightly with pulse durations longer than 900 time units.

D. Dissociation using the Optimized Pulse. In an effort to improve on the performance of the linearly chirped pulses, we built a simple optimization algorithm to construct pulses of arbitrary form. This was done by choosing n discrete values of the envelope function $U(t_m)$ in eq 7, $m = 1, 2, ..., n$, as variational parameters and formulating a cost function which numerically evaluated the effectiveness of the pulse. Factors such as final bond energies, the average fluence of the laser, the presence of transients, etc., were all included in the cost function. The relative importance of all these factors was controlled by multiplicative factors which were adjusted a posteriori to ensure the best results. This cost function was minimized by iteratively adjusting the form of the electric field pulse, using a modified gradient search algorithm. The minimization was considered complete when further iterations and adjustments of the pulse did not continue to decrease the cost function significantly. The resulting final form of the electric field pulse was then considered as the optimal pulse. Our method has limitations and it cannot handle long pulses. However, our goal here is modest: we wish to find a laser pulse that could selectively break the C−N bond in HCN leaving the C−H bond intact, and we are not looking for maximally optimized results which can be obtained by more sophisticated methods.[26,36]

We studied the performance of optimized pulses in the dissociation of both the C−H and C−N bonds. Due to computational limitations, we were only able to study relatively short pulses, with duration up to about 120 time units (0.18 ps), and all computation was performed for one trajectory only. On this short time scale, excitation can successfully compete with IVR. In Figure 8, we show a representative result for the selective dissociation of the C−H bond with an optimized pulse of 63 time units in length. Plotted as functions of time are the individual bond energies, the total energy of the system, and

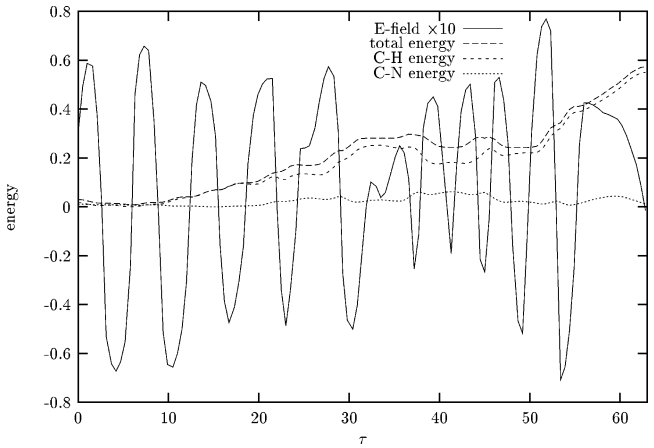

Figure 8. Response of the molecule to a pulse optimized for dissociating the C−H bond. The initial oscillations of the electric field have frequency approximately resonant with the harmonic frequency of the bond.

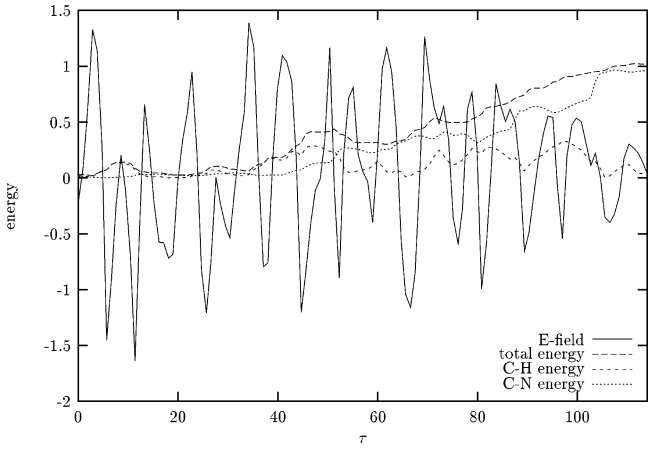

Figure 9. Response of the molecule to a pulse optimized for dissociating the C−N bond. The stronger C−N bond requires a longer pulse to dissociate.

the electric field, all in dimensionless units. For clarity, the scale of the dimensionless electric field, ϵ_L, has been expanded by a factor of 10. ϵ_L is related to the instantaneous intensity of the radiation by $I(\tau) = \epsilon_L(\tau)^2 I_0 = [\epsilon_L(\tau)]^2 \times 108.5 \times 10^{13}$ W/cm^2, so that an intensity of 1 TW/cm^2 corresponds to $\epsilon_L = 0.0096$. The optimal pulse shows fairly smooth behavior, and the intentity is generally in the low to mid 10^{14} W/cm^2 range. It shows some sinusoidal oscillations, the frequency of which (at least initially) approximates the harmonic frequency of the C−H bond. However, as time progresses, the oscillations become more complicated. In the range $35 < \tau < 55$, the pulse changes form abruptly and exhibits behavior similar to upward chirping. Perhaps this additional and unexpected complexity is required for the suppression of the IVR. In any case, this behavior becomes more pronounced if the pulse is made longer, and additionally, transient spikes in the field begin to appear.

Figure 9 shows an optimized pulse which dissociates the C−N bond. Note that the dimensionless dissociation energy for this bond is about 0.96, and the C−N bond energy indeed reaches this value at the end of the pulse. A pulse of duration 114 time units gave the best results. Given the longer response times of the C−N bond relative to the C−H, it is not unexpected that a longer pulse would perform better in this case. As expected, the peak electric intensities for the C−N bond dissociation are larger than those required for the C−H bond: they are on the order of 10^{15} W/cm^2, which undoubtly would ionize the molecule, a process that we do not study in this paper.

V. Conclusions

Our research on this project has, we believe, shed some light on the problem of selective control of bonds of HCN and linear triatomic molecules in general. The overall trends in the quest for control are quite clear: it is relatively straightforward to control the weaker bond, whereas it is quite difficult to control the stronger bond, unless we confine ourselves to very low excitation levels or else utilize ultra short, very intense laser pulses. The single confounding factor here is internal vibrational redistribution (IVR). At low excitation levels, IVR is slow, and it does not interfere with our controlling efforts. It is possible to highly excite and dissociate the weaker bond despite IVR. Even here, ample energy leakage into the stronger bond occurs during the excitation process, but the energy levels attained by the stronger bond are well below its dissociation levels. We found that simple linearly chirped pulses work well in exciting the weaker bond when the laser parameters are properly chosen: an initial frequency that is in resonance with the initial state frequency of the bond, a sufficiently slow chirp rate, and a sufficiently high intensity. These findings are qualitatively in agreement with the predictions of bucket dynamics theory for diatomic molecules.[21,32] If efficient dissociation is the goal, an excited C−H bond should be fairly easy to break with the application of a second laser of constant frequency immediately after the chirped pulse.

We found that the C−N bond also responds to simple chirped pulses, albeit the required intensities are higher and the chirping rates lower, so that a more intense ($\sim 10^{14}$ W/cm^2) and longer pulse (of duration 5 ps or more) is needed. However, it is not possible to dissociate the C−N bond this way, because IVR transfers enough energy to the C−H bond to break it first. The characteristic time scale of the IVR is about 0.1 ps, which is about 50 times shorter than the shortest effective chirped pulse.

Our investigation of short (less than 0.5 ps) optimized pulses revealed that both bonds, in principle, can be dissociated in this manner. However, the electric fields required are on average about 1×10^{14} W/cm^2, which might well ionize the molecule before dissociation occurs. The major shortcoming of our study is not being able to model the electronic motion, which has significant effects on the behavior of the molecule when it is exposed to electric fields with intensities $\sim 10^{14}$ W/cm^2. Modeling both the electronic and nuclear dynamics is very difficult and has only been carried out for the simplest molecules.[37,38] Given the encouraging results of our limited optimization scheme, a more sophisticated optimizer could have been built. However, the main goal of this paper is to study the dynamics of selective excitation of HCN by simple chirped pulses, and we are content with demonstrating that the stronger C−N bond can be broken with an optimized pulse. The field of manipulation and control of molecules by externally applied laser pulses is a fruitful area for active development in the future.

Acknowledgment. We thank the Natural Sciences and Engineering Research Council (NSERC) of Canada for financial support.

References and Notes

(1) Zare, R. N. *Science* **1998**, *279*, 1875.
(2) Warren, W. S.; Rabitz, H.; Dahleh, M. *Science* **1993**, *259*, 1581.
(3) Rabitz, H.; de Vivie-Riedle, R.; Motzkus, M.; Kompa, K. *Science* **2000**, *288*, 824.

(4) Levis, R. J.; Menkir, G. M.; Rabitz, H. *Science* **2001**, *292*, 709.
(5) Weinachit, T. C.; Bartels, R.; Backus, S.; Bucksbaum, P. H.; Pearson, B.; Geremia, J. M.; Rabitz, H.; Kapteyn, H. C.; Murnane, M. M. *Chem. Phys. Lett*. **2001**, *344*, 333.
(6) Maas, D. J.; Duncan, D. I.; van der Meer, A. F. G.; van der Zande, W. J.; Noordam, L. D. *Chem. Phys. Lett*. **1997**, *270*, 45.
(7) Maas, D. J.; Duncan, D. I.; Vrijen, R. B.; van der Meer, A. F. G.; Noordam, L. D. *Chem. Phys. Lett*. **1998**, *290*, 75.
(8) Maas, D. J.; Vrakking, M. J. J.; Noordam, L. D. *Phys. Rev. A* **1999**, *60*, 1351.
(9) Windhorn, L.; Witte, T.; Yeston, J.; Proch, D.; Motzkus, M.; Kompa, K.; Fuss, W. *Chem. Phys. Lett*. **2002**, *357*, 85.
(10) Witte, T.; Hornung, T.; Windhorn, L.; Proch, D.; de Vivie-Riedle, R.; Motzkus, M.; Kompa, K. J. *Chem. Phys*. **2003**, *118*, 2021.
(11) Chelkowski, S.; Bandrauk, A. D.; Corkum, P. B. *Phys. Rev. Lett*. **1990**, *65*, 9355.
(12) Chelkowski, S.; Bandrauk, A. D. *Chem. Phys. Lett*. **1991**, *186*, 264.
(13) Krempl, S.; Eisenhammer, T.; Hiibler, A.; Mayer-Kress, G.; Milonni, P. W. *Phys. Rev. Lett*. **1992**, *69*, 430.
(14) Just, B.; Manz, J.; Trisca, I. *Chem. Phys. Lett*. **1992**, *193*, 423.
(15) Korolkov, M. V.; Paramonov, G. K.; Schmidt, B. *J. Chem. Phys*. **1996**, *105*, 1862.
(16) Korolkov, M. V.; Manz, J.; Paramonov, G. K. *Chem. Phys*. **1997**, *217*, 341.
(17) Korolkov, M. V.; Paramonov, G. K. *Phys. Rev. A* **1997**, *56*, 3860.
(18) Andrianov, I. V.; Paramonov, G. K. *Phys. Rev. A* **1999**, *59*, 2134.
(19) Oppel, M.; Paramonov, G. K. *Phys. Rev. A* **1999**, *60*, 3663.
(20) Martin, R.; Kim, J.-H.; Liu, W.-K.; Yuan, J.-M. *J. Chin. Chem. Soc*. **2002**, *49*, 757.
(21) Liu, W.-K.; Wu, B.; Yuan, J.-M. *Phys. Rev. Lett*. **1995**, *75*, 1292.
(22) Morse, P. M. *Phys. Rev*. **1929**, *34*, 57.
(23) Heagy, J. F.; Lu, Z.-M.; Yuan, J.-M.; Vallieres, M. In *Quantum Non-Integrability*; Feng, D., Yuan, J.-M., Eds.; World Scientific: Singapore, 1992.
(24) Chelkowski, S.; Bandrauk, A. D. In *Coherence Phenomena in Atoms and Molecules in Laser Fields*; Bandrauk, A., Ed.; Plenum: New York, 1992; Vol. 287, pp 333−347, NATO ASI Series B.
(25) Matusek, D. R.; Ivanov, M. Y.; Wright, J. S. *Chem. Phys. Lett*. **1998**, *284*, 247.
(26) Botina, J.; Rabitz, H.; Rahman, N. *J. Chem. Phys*. **1995**, *102*, 226, 4687.
(27) Balling, P.; Maas, D. J.; Noordam, L. D. *Phys. Rev. A* **1994**, *50*, 4276.
(28) Hasbani, R.; Ostojic, B.; Bunker, P. R.; Ivanov, M. Y. *J. Chem. Phys*. **2002**, *116*, 10636.
(29) Friedrich, B.; Herschbach, D. *Phys. Rev. Lett*. **1995**, *74*, 4623.
(30) Dion, C. M.; Chelkowski, S.; Bandrauk, A. D.; Umeda, H.; Fujimura, Y. *J. Chem. Phys*. **1996**, *105*, 9083.
(31) Botschwina, P. *Chem. Phys*. **1983**, *81*, 73.
(32) Yuan, J.-M.; Liu, W.-K. *Phys. Rev. A* **1998**, *57*, 1992.
(33) Percival, I. C. *Adv. Chem. Phys*. **1977**, *36*, 1.
(34) Gu, Y.; Yuan, J.-M. *Phys. Rev. A* **1987**, *36*, 3788.
(35) Press, W. H.; Teukolsky, S. A.; Vetterling, W. T.; Flannery, B. P. *Numerical Recipes in FORTRAN: the Art of Scientific Computing*, 2nd ed.; Cambridge University Press: New York, 1992.
(36) Umeda, H.; Fujimura, Y. *J. Chem. Phys*. **2000**, *113*, 3510.
(37) Walsh, T. D. G.; Ilkov, F. A.; Chin, S. L.; Chateauneuf, F.; Nguyen-Dang, T. T.; Chelkowski, S.; Bandrauk, A. D. *Phys. Rev. A* **1998**, *58*, 3922.
(38) Chelkowski, S.; Zamojski, M.; Bandrauk, A. D. *Phys. Rev. A* **2001**, *63*, 023409.